



Ferromagnetism and Electronic Structure of (Ga,Mn)As:Bi and (Ga,Mn)As Epitaxial Layers

O. Yastrubchak^{1,*}, J. Sadowski^{2,3}, T. Andrearczyk³, J. Z. Domagała³, Ł. Gluba¹,
 M. Rawski⁴, J. Żuk¹, T. Wosinski³

¹ *Institute of Physics, Maria Curie-Skłodowska University in Lublin, Pl. M. Curie-Skłodowskiej 1, 20-031 Lublin, Poland*

² *MAX-IV Laboratory, Lund University, P.O. Box 118, SE-221 00 Lund, Sweden*

³ *Institute of Physics, Polish Academy of Sciences, Al. Lotników 32/46, 02-668 Warsaw, Poland*

⁴ *Analytical Laboratory, Maria Curie-Skłodowska University in Lublin, Pl. M. Curie-Skłodowskiej 3, 20-031 Lublin, Poland*

(Received 19 June 2013; published online 30 August 2013)

The photoreflectance (PR) spectroscopy was applied to study the band-structure in GaAs:Bi, (Ga,Mn)As and (Ga,Mn)As:Bi layers with the 4% of Mn and 1 % of Bi content and, as a reference, undoped GaAs layer. All films were grown by low temperature (LT) MBE on semi-insulating (001) GaAs substrates. Photoreflectance studies were supported by Raman spectroscopy and high resolution X-ray diffractometry (XRD) measurements. Magnetic properties of the films were characterized with a superconducting quantum interference device (SQUID) magnetometer. Our findings were interpreted in terms of the model, which assumes that the mobile holes residing in the valence band of GaAs and the Fermi level position determined by the concentration of valence-band holes.

Keywords: (Ga,Mn)As:Bi, (Ga,Mn)As, Diluted ferromagnetic semiconductor, Photoreflectance (PR) spectroscopy, Fermi level, Band-structure.

PACS numbers: 75.50.Pp;71.20.Nr;75.30.-m;78.20.Jq

1. INTRODUCTION

The GaAs semiconductor alloy compounds containing Bi or Mn have emerged as potential candidates for novel photonic and spintronic applications. The band gap of the GaAs:Bi epitaxial layers is red shifted considerably upon the addition of only a few atomic percent of Bi and exhibits other anomalous properties, such as a reduced temperature dependence as well as giant spin-orbit splitting. These effects are very useful in solar cells as well as in optical telecommunication and the internet underpinned by the development of semiconductor lasers emitting at 1.3 μm and at 1.55 μm , the wavelengths at which, respectively, the dispersion is zero and losses are minimized in standard optical fibers. To explain these unusual features of the electronic structure of the GaAs:Bi epitaxial layers the band anticrossing (BAC) model was developed [1]. According to this model the hybridization of the extended p-like states comprising the valence band of the GaAs host semiconductor with the close-lying localized p-like states of Sb or Bi leads to a nonlinear shift of the valence-band edge and a reduction of the band gap.

The ternary III-V semiconductor (Ga,Mn)As has attracted a lot of attention as the model diluted ferromagnetic semiconductor, combining semiconducting properties with magnetism. There are two alternative models of the band structure of (Ga,Mn)As. The first one assumes mobile holes residing in the valence band of GaAs and the Fermi level position determined by the concentration of valence-band holes [2,3]. The second one involves persistence of the narrow, Mn-related, impurity band in highly Mn-doped (Ga,Mn)As with metallic conduction. In this model the Fermi level ex-

ists in the impurity band within the band gap and the mobile holes retain the impurity band character [4]. It was suggested in [5], that in the (Ga,Mn)As the valence band anticrossing interaction is observed as well.

We have presented in [6,7,8] the results of our investigations the electronic- and band-structure properties of (Ga,Mn)As epitaxial layers with a low Mn content, in the range from 0 to 1.2% where the onset of ferromagnetic ordering occurs, and a high Mn content [6], in the range up to 6% where (Ga,Mn)As epitaxial layers have high Curie temperature (T_c), by applying modulation photoreflectance spectroscopy and several complementary characterization techniques such as high-resolution X-ray diffractometry, thermoelectric power, Raman spectroscopy and SQUID magnetometry. PR spectroscopy results presented in [7,8] were elaborated by performing both the full-line-shape analysis of the PR spectra and the analysis of the periods of Franz-Keldysh oscillations, which concluded with similar findings on the evolution of the optical transition energies with increasing Mn content in the layers. Decrease in the band-gap-transition energy, with respect to that in the reference LT-GaAs layer, was revealed in very low-doped (Ga,Mn)As layer with Mn content of 0.001% -0.005% and *n*-type conductivity. It is interpreted by assuming a merging of the Mn-related impurity band with the host GaAs valence band resulting in electronic transitions from the top of this disordered valence band to the conduction band. On the other hand, an increase in the band-gap-transition energy (E_0) with increasing Mn content was observed in (Ga,Mn)As layers with higher Mn content of 0.8% and 1.2%, displaying p-type conductivity. It is interpreted

* yastrub@hektor.umcs.lublin.pl

as a result of the Moss-Burstein shift of the absorption edge due to the Fermi level position, determined by the free-hole concentration, within the valence band.

In *p*-type (Ga,Mn)As with 1–2% of Mn content and hole density close to that of the metal-insulator transition (MIT), the interband transition energy was blue shifted with respect to that in reference LT-GaAs. On the other hand, a substantial red shift, of 40 meV, of the E_0 energy was revealed in (Ga,Mn)As with the highest (6%) Mn content and a hole density corresponding to metallic side of the MIT. These results, together with the determined other parameters of the interband electro-optic transitions near the center of the Brillouin zone, which were significantly different from those in reference LT-GaAs, was interpreted in terms of a disordered valence band, extended within the band-gap, formed in highly Mn-doped (Ga,Mn)As as a result of merging the Mn-related impurity band with the host GaAs valence band.

The experimental results presented in our previous study are consistent with the valence-band origin of mobile holes, which mediate ferromagnetic ordering in the (Ga,Mn)As diluted ferromagnetic semiconductor. The disordered character of the valence band may account for the observed very low mobility of holes in ferromagnetic (Ga,Mn)As layers.

Considering the above, the electronic structure of the more complex semiconductor alloy compounds such as (Ga,Mn)As:Bi could be very complicated. Nevertheless, we have expected that the understanding of this issue allow to anticipate band structure of the new materials and to design complex semiconductor alloy compounds with unusual properties.

2. SUPLES AND EXPERIMENTAL PROCEDURES

We have investigated GaAs:Bi, (Ga,Mn)As, (Ga,Mn)As:Bi layers with 4% of Mn and 1% of Bi content and, as a reference, undoped GaAs layer, grown by LT-MBE at a temperature of 230°C. All the epitaxial layers were grown pseudomorphically on semi-insulating (001) GaAs substrates. The alloy compositions were determined from high resolution X-ray diffractometry (XRD) measurements. The photoreflectance (PR) spectroscopy enabled the determination of the band gap values (E_0). Both the Mn composition and the film thickness were verified during the growth by the reflection high-energy electron diffraction (RHEED) intensity oscillations, which enabled to determine the composition and film thickness with accuracy of 0.1% and one monolayer, respectively. The quality of the epitaxial layers were confirmed in transmittance electron microscope (TEM).

The films were subjected to investigations of their properties using several complementary characterization techniques. Magnetic properties and the T_C values for the (Ga,Mn)As films were inspected using both magnetic-field- and temperature-dependent SQUID magnetometry. Micro-Raman spectroscopy was employed to estimate the hole densities in the thick (Ga,Mn) As films. The micro-Raman measurements were performed using an inVia Reflex Raman micro-

scope (Renishaw) at room temperature with the 514.5-nm argon ion laser line as an excitation source. Structural properties of the thick epitaxial films were investigated by analysis of XRD results obtained at the temperature 27°C by means of high-resolution X-ray diffractometer equipped with a parabolic X-ray mirror and four-bounce Ge 220 monochromator at the incident beam and a three-bounce Ge analyzer at the diffracted beam. Misfit strain in the epitaxial films was investigated using the reciprocal lattice mapping and the rocking curve techniques for both the symmetric 004 and asymmetric 224 reflections of Cu $K\alpha_1$ radiation.

Room temperature PR measurements were performed using an helium-cadmium ion laser working at the 442 nm wavelength and a nominal power of 20 mW as a pump-beam source and a 250 W halogen lamp coupled to a monochromator as a probe-beam source. The PR signal was detected by a Si photodiode. The chopping frequency of the pump beam was 70 Hz and the nominal spot size of the pump and probe beams at the sample surface were 2 mm in diameter.

3. RESULTS AND DISCUSSION

3.1 Structural and magnetic characterization

High-resolution XRD measurements have shown that all the epitaxial layers were grown pseudomorphically on GaAs substrate under compressive misfit strain. The layers exhibited a high structural perfection, as proved by clear X-ray interference fringes revealed for the 004 Bragg reflections of all the layers, as shown in figure 1. The layer thicknesses calculated from the angular spacing of the fringes correspond very well to their thicknesses determined from the growth parameters. Diffraction peaks corresponding to the GaAs:Bi, (Ga,Mn)As, (Ga,Mn)As:Bi films in figure 1 shift to smaller angles, with respect to that of the GaAs substrate, as a result of larger lattice parameters. In LT-GaAs it is caused by incorporation of a large amount of about 1% excess arsenic, mainly in form of arsenic antisites, As_{Ga} [9]. The lattice parameter in all epitaxial layers becomes more increased as a result of additional incorporation of the Bi_{As} , Mn_{Ga} and Mn_{I} atoms in the crystal lattice [10]. Angular positions of the diffraction peaks corresponding to epitaxial layers were used to calculate the perpendicular lattice parameters, c , and the relaxed lattice parameters, a_{rel} , [11] (assuming the epitaxial layer elasticity constants to be the same as for GaAs). The lattice unit of the layers changes with increasing lattice mismatch from the zincblende cubic structure to the tetragonal structure with the perpendicular lattice parameter larger than the lateral one, equal to the GaAs substrate lattice parameter, which is $a_{sub} = 5.65349\text{\AA}$ in our XRD experiments. The decrease in angular positions of the diffraction peak from the epitaxial layers results in a increase in their lattice parameters, which is in agreement with the expected value of Mn and Bi doping [10].

The TEM cross-sectional image of the GaAs:Bi presented in figure 2 has proved the structural perfection of this epi-layers and allowed to check the its lattice parameters in the grown direction [001].

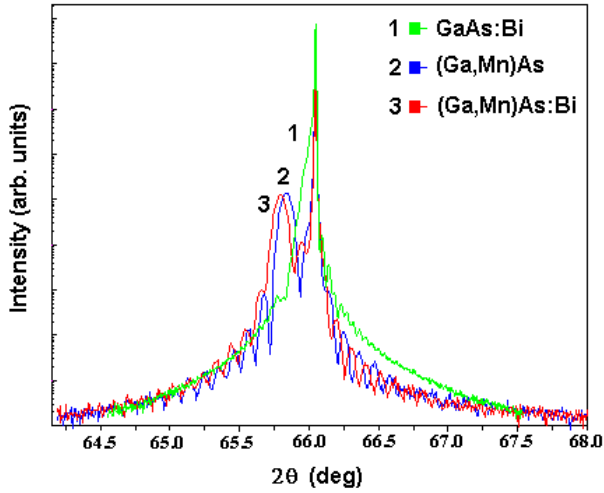


Fig. 1 – High-resolution X-ray diffraction spectra: $2\theta/\omega$ scans for (004) Bragg reflections for (1) GaAs:Bi, (2) (Ga,Mn)As and (3) (Ga,Mn)As:Bi epitaxial layers grown on (001) semi-insulating GaAs substrate. The narrow line corresponds to reflection from the GaAs substrate and the broader peaks at lower angles are reflections from the layers.

The results of SQUID magnetometry applied to the (Ga,Mn)As and (Ga,Mn)As:Bi layers are presented in figure 3. They show that the layers exhibit an in-plane easy axis of magnetization, characteristic of compressively strained (Ga,Mn)As layers, and well defined hysteresis loops in their magnetization vs. magnetic field dependence shown in the insets in figure 3. The as-grown layers displayed the similar T_C values of 50-60K.

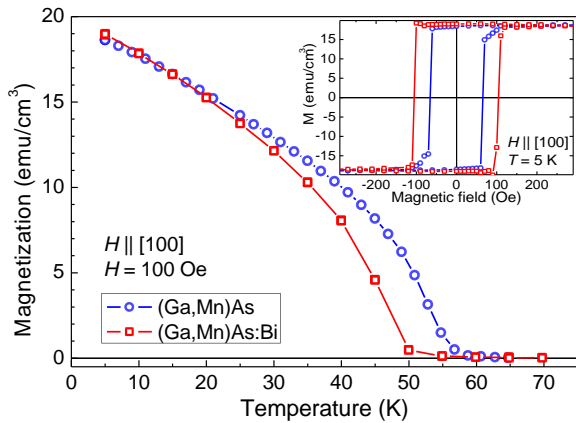


Fig. 3 – SQUID magnetization along the in-plane [110] crystallographic direction vs. temperature for the as-grown (Ga,Mn)As and (Ga,Mn)As:Bi layers after subtraction of diamagnetic contribution from the GaAs substrate. Magnetization hysteresis loops measured at a temperature of 5 K are shown in the insets

3.2 Micro-Raman characterization

Quantitative analysis of Raman spectra can provide important information about the free-carrier density. Seong et al. [12] proposed a powerful procedure, which enables for accurate determining the carrier density without necessity of applying large magnetic fields, as is required in the Hall-effect measurements for ferromagnetic materials.

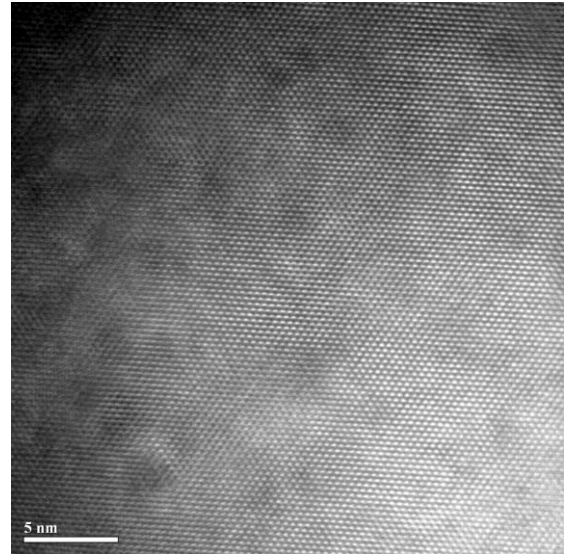


Fig. 2 – Cross-sectional image of the GaAs:Bi epitaxial layer obtained using TEM microscope.

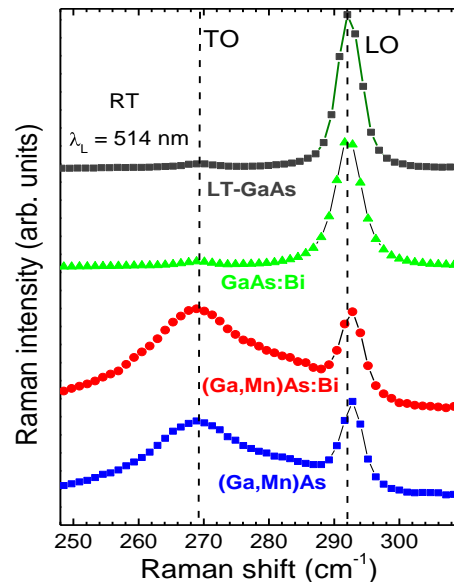


Fig.4 – Raman spectra recorded at room temperature in backscattering configuration from the (001) surfaces of the LT-GaAs reference film and two 230-nm (Ga,Mn)As films. The spectra have been vertically offset for clarity. The dashed lines indicate the positions of the Raman LO- and TO-phonon lines for the LT-GaAs reference film

In (Ga,Mn)As films, characterized by a high density of free holes of about 10^{20} cm^{-3} , the interaction between the hole plasmon and the LO phonon leads to the formation of coupled plasmon-LO phonon (CPLP) mode [13]. In addition, it results in a broadening and a shift of the Raman line from the LO-phonon position to the TO-phonon position depending on the hole density [14]. From micro-Raman spectra we have estimated the hole concentrations of $1.5 \times 10^{20} \text{ cm}^{-3}$ in both the (Ga,Mn)As and (Ga,Mn)As:Bi films. The obtained results suggest that these two epi-layers are metallic-like *p*-type materials with the similar magnetic properties.

3.3 Photoreflectance spectroscopy

The PR spectra measured for LT-GaAs, GaAs:Bi, (Ga,Mn)As:Bi and (Ga,Mn)As epitaxial layers in the photon-energy range from 1.3 to 1.7 eV (Fig. 5) revealed a rich, modulated structure containing electric-field-induced Franz-Keldysh oscillations (FKO) at energies above the fundamental absorption edge. The modulation mechanism of the feature around the interband transition energy (peaks A) observed for (Ga,Mn)As:Bi and (Ga,Mn)As epitaxial layers results from the thermal excitation of impurities or traps at the layer/substrate interface and their momentary re-filling by the laser-injected carriers [15]

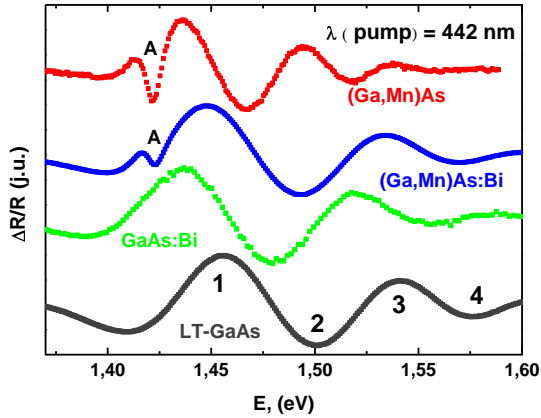


Fig. 5 – Sequence of the photoreflectance spectra for the as-grown LT-GaAs, GaAs:Bi, (Ga,Mn)As:Bi and (Ga,Mn)As film epitaxially grown on GaAs substrate (dots). The spectra have been vertically offset for clarity

The energy values E_g connected with the interband transition energy E_0 are obtained for all epitaxial layers (see Fig.6) from the intersection with the ordinate of the linear dependence of the energies of FKO extrema E_m vs. their “effective index” defined as $F_m = [3\pi(m - 1/2) / 4]^{2/3}$:

$$E_m = E_g + \hbar\theta F_m \quad (1)$$

where m is the extremum number (marked on Fig. 5) and $\hbar\theta$ – the electro-optic energy defined as $\hbar\theta = e^2 \hbar^2 F^2 / 2\mu^{1/3}$, F is the electric field and μ is the interband reduced effective mass.

Our PR results evidence a tangible difference in the electronic band structures of LT-GaAs, GaAs:Bi, (Ga,Mn)As:Bi and (Ga,Mn)As epitaxial layers. The significant red shift, of 20 meV, of E_g transition in the GaAs:Bi film with respect to LT-GaAs epi-layer even for very low Bi concentration (1%) indicates the reduction of the band gap in the GaAs:Bi because of BAC.

On the other hand, small red shift of the E_g transitions in the (Ga,Mn)As and (Ga,Mn)As:Bi films with 4% of Mn contents are consistent with the band structure model, where the Mn-related impurity band is merged with the GaAs valence band, forming a disordered valence band extended within the band gap.⁶ In

this case the E_g transition occurs from the Fermi level in the disordered valence band to the conduction band. The lack of splitting of the PR spectra into light- and heavy-hole features in the spectral area near the E_g transition, even in the (Ga,Mn)As:Bi film with a vertical strain as high as 3×10^{-3} (from XRD results), may be explained by the disordered character of valence band.

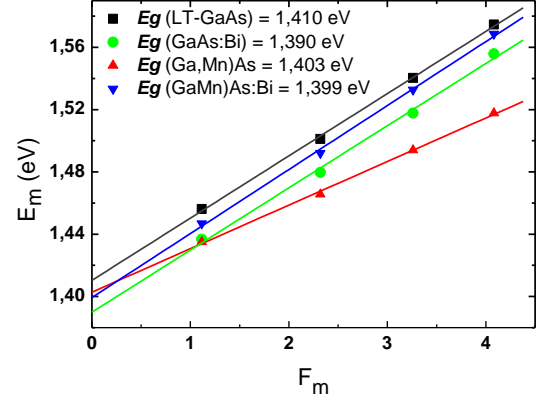


Fig. 6 – Analysis of the period of Franz-Keldysh oscillations for LT-GaAs, GaAs:Bi, (Ga,Mn)As:Bi and (Ga,Mn)As. The values of E_g obtained from the analysis are listed in the figure. The numbers of the FKO extrema used for the analysis are marked on Fig. 5

Assuming the large concentration of the free holes (up to $1.5 \times 10^{20} \text{ cm}^{-3}$ for the (Ga,Mn)As and (Ga,Mn)As:Bi films) reside in the valence band, we have expected the significant blue shift of the band gap because of the Burstein-Moss effect. Nevertheless, the coupling of the free carriers in the band states with impurities (especially Mn interstitials) leads to an upward shift of the valence-band edge, resulting in a reduction of the band gap. The band gap renormalization associated with the change in the lattice parameters (observed in HR-XRD) as well as with the high density of free holes (observed by micro-Raman) also lead to a small reduction in the band-gap energy for these epilayers [16].

The significant reduction of the band gap for the GaAs:Bi caused by the hybridization of the extended p -like states comprising the valence band of the GaAs host with the close-lying localized p -like states of Bi, is not observed in the (Ga,Mn)As:Bi probably because of the large valence-band distortion.

ACKNOWLEDGEMENTS

OY acknowledges financial support from the Foundation for Polish Science under Grant POMOST/2010-2/12 sponsored by the European Regional Development Fund, National Cohesion Strategy: Innovative Economy. This work was also supported by the Polish Ministry of Science and Higher Education under Grant No. N N202 129339. The MBE project at MAX-IV Laboratory is supported by the Swedish Research Council (VR).

REFERENCES

1. K. Albery, J. Wu, W. Walukiewicz, K. M. Yu, O.D. Dubon, S.P. Watkins, C.X. Wang, X. Liu, Y.-J. Cho, and J. Furdyna, *Phys. Rev. B* **75** No4, 045203 (2007).
2. T. Dietl, H. Ohno, F. Matsukura, J. Cibert, D. Ferrand, *Science* **287**, 1019 (2000).
3. T. Dietl, *Nature Materials* **9**(12), 965-974 (2010).
4. Shinobu Ohya, Kenta Takata, Masaaki Tanaka, *Nature Physics* **7**, 342 (2011).
5. K. Alberi, K.M. Yu, P.R. Stone, O.D. Dubon, W. Walukiewicz, T. Wojtowicz, X. Liu, J.K. Furdyna, *Phys. Rev. B* **78**, 075201 (2008).
6. O. Yastrubchak, J. Zuk, H. Krzyzanowska, J.Z. Domagala, T. Andrearczyk, J. Sadowski and T. Wosinski, *Phys. Rev. B* **83**, 245201 (2011).
7. O. Yastrubchak, *J. Nano- Electron. Phys.*, **4** No1, 01016 (2012).
8. O. Yastrubchak, J. Żuk, L. Gluba, J.Z. Domagala, J. Sadowski, T. Wosinski, *Proceedings 1-st NAP; Nanomaterials: Applications and Properties*; **1**, 328 (2011).
9. D. C. Look, D. C. Walters, M. O. Manasreh, J. R. Sizelove, C. E. Stutz and K. R. Evans, *Phys. Rev. B* **42**, 3578 (1990).
10. I. Kuryliszyn-Kudelska, J. Z. Domagala, T. Wojtowicz, X. Liu, E. Łusakowska, W. Dobrowolski, J. K. Furdyna, *J. Appl. Phys.* **95**, 603 (2004).
11. O. Yastrubchak, J. Bak-Misiuk, E. Łusakowska, J. Kaniewski, J. Z. Domagala, T. Wosinski, A. Shalimov, K. Regini, A. Kudla, *Physica B-Condensed Matter*. **340**, 1082 (2003).
12. M.J. Seong, S.H. Chun, H.M. Cheong, N. Samarth, and A. Mascarenhas, *Phys. Rev. B* **66**, 033202 (2002).
13. G. Irmer, M. Wenzel, and J. Monecke, *Phys. Rev. B* **56**, 9524 (1997).
14. W. Limmer, M. Glunk, W. Schoch, A. Köder, R. Kling, R. Sauer, and A. Waag, *Physica E* **13**, 589 (2002).
15. M. Sydor, J. Angelo, J.J. Wilson, W.C. Mitchel, and M.Y. Yen, *Phys. Rev. B* **40**, 8473 (1989).
- T. de Boer, A. Gamouras, S. March, V. Novak, and K.C. Hall, *Phys. Rev. B* **85**, 033202 (1997).